

Short-Term Dielectric Performance Assessment of BOPP Capacitor Films: A Baseline Study

I. Rytöluoto, M. Ritamäki & K. Lahti
Laboratory of Electrical Energy Engineering
Tampere University of Technology
Tampere, Finland

Abstract—This paper examines the morphology and short-term dielectric performance of commercial capacitor BOPP films, with the purpose of serving as an industrial reference in European project GRIDABLE in which next-generation PP-silica nanocomposite materials are developed for DC capacitor and cable applications. Results from dielectric spectroscopy, thermally stimulated depolarization current (TSDC) and DC conductivity measurements are reported, providing insight into the dielectric loss behavior and charge trapping/transport properties of the studied films. Comprehensive short-term dielectric breakdown strength analysis using small- and large-area approaches indicates high dielectric breakdown performance, even at an elevated temperature of 100 °C.

I. INTRODUCTION

Recent trends towards wider adaptation of high-voltage direct current (HVDC) technologies in smart grids and the continually increasing demand for higher capacitive energy density in e.g. voltage-source converters (VSC) have set stringent demands for the dielectric performance and long-term reliability of film capacitors under high electrical and thermal stresses. Enhancement of dielectric and thermal characteristics of biaxially oriented polypropylene (BOPP) film, the current industry standard of polymeric film capacitor dielectrics, is thus required. Along with the recent developments towards super clean electrical-grade high-isotactic base polypropylene (PP) and optimization of film processing and morphology, alternative strategies through incorporation of nanoparticles are actively investigated to enhance the performance of the current capacitor-grade PP materials. This study examines the morphology and short-term dielectric performance of commercial metallized and non-metallized capacitor BOPP films based on high purity isotactic polypropylene homopolymer. These results, which evidence the high dielectric performance of the studied state-of-the-art capacitor BOPP films, serve as an industrial reference in the European project GRIDABLE, which aims to develop next-generation PP-silica nanocomposite materials with enhanced dielectric performance for both DC capacitor and cable applications.

II. EXPERIMENTAL

A. Material specifications and characterization

Commercial Zn/Al-metallized and non-metallized (base) BOPP capacitor films manufactured by the tenter frame process were studied. For each film type, two thickness variants, namely 5 μm and 10 μm , were obtained. All the films were manufactured using the same base polymer, a capacitor-grade isotactic polypropylene homopolymer with high purity and low ash content. Thermal characteristics, crystalline morphology and surface/cross-sectional structure of the films

were analyzed by differential scanning calorimetry (DSC), optical microscopy (OM) and 3D optical profilometry.

B. Dielectric breakdown characterization

Comprehensive short-term dielectric breakdown strength assessment was performed for each BOPP film using (i) large-area multi-breakdown methodology and (ii) conventional small-area single-breakdown methodology under both DC and AC ramp voltages. Details on the utilized large-area multi-breakdown and small-area single breakdown measurement methods are presented elsewhere [1], [2], and thus, for the sake of brevity, are not repeated here. In addition to room temperature measurements, additional high temperature large-area DC multi-breakdown measurements were also performed at 100 °C (± 1.5 °C) using a system recently presented in [3]. Table I summarizes the temperature T , active area A , sample size N and total film area A_{tot} for each measurement. Breakdown data were analyzed using Weibull statistics.

C. Dielectric spectroscopy, TSDC and DC conductivity measurements

For dielectric spectroscopy, TSDC and conductivity measurements, electrodes (\varnothing 22 mm) were deposited on both sides of the BOPP sample films using a custom-built e-beam evaporator (Instrumentti Mattila) inside a clean room facility. The deposited materials were either Ni+Au (10 nm + 100 nm) or Al (100 nm). High vacuum (pressure $< 1 \times 10^{-6}$ mbar) and low deposition rate (0.05–0.20 nm/s) were maintained during the evaporation process to minimize thermal and radiative damaging of the sample film. Prior to electrical measurements, the evaporated samples were short-circuited and stored in vacuumed desiccator for several days in an attempt to remove residual charge which may had been injected during the evaporation. For some of the samples this was done at an elevated temperature (70 °C).

Complex relative permittivity $\epsilon_r^* = \epsilon_r + i\epsilon_r'$ was measured as a function of frequency and temperature using a Novocontrol Alpha-A dielectric analyzer equipped with a Novocool temperature control system and a shielded BDS-1200 sample cell (1 V_{AC,rms}). For TSDC and DC conductivity measurements, a high voltage DC source, a shielded sample cell equipped with a PT100 temperature sensor (Novocontrol BDS1200 HV sample cell) and an electrometer (Keithley 6517B) were utilized. For voltages up to 1 kV, the built-in DC voltage source of Keithley 6517B was utilized, while for higher voltages a Keithley 2290E-5 DC power supply was used. An overload protection circuit along with a series resistor was used to protect the electrometer in case of sample breakdown during voltage application. Temperature control was realized using the Novocool system or a PID-controlled electrical heating element.

For thermally stimulated depolarization current measurements, the procedure was as follows:

- 1) Sample is heated to $T_p = 80$ °C.
- 2) Sample is held isothermally and DC voltage is applied for $t_p = 40$ min (charging).
- 3) Temperature is rapidly decreased to $T_0 = -50$ °C and maintained isothermally for 5 min (voltage still applied).
- 4) Voltage is removed; sample is short-circuited through the electrometer and maintained isothermally for 3 min.
- 5) Sample is heated at a linear rate of $\beta = 3.0$ °C/min up to $T_{max} = 125$ °C while recording the depolarization current.

DC conductivity measurements were performed at temperatures of 30 °C, 70 °C and 100 °C under electric fields of 30–250 V/μm. At each electric field magnitude, the voltage application time was 20–24 h, after which the sample was let to relax at the set temperature. For each temperature, same sample was used for the next higher electric field (unless specified otherwise), similarly as e.g. in [4].

III. RESULTS AND DISCUSSION

A. Film structure and morphology

DSC measurements performed on the 10 μm base-BOPP film indicated a melting temperature T_m of ~167.9 °C, a glass-transition temperature T_g of approx. -5.4 °C and an initial crystallinity X_{DSC} of ~61 % (assuming $\Delta H^0_a = 209$ g/J for the heat of fusion of a completely crystalline α -form iPP material). The BOPP film 1st heating endotherm corresponded to that of a monoclinic α -form crystalline structure, showing no traces of hexagonal β -form, as is typical for biaxially stretched film [5]. Optical microscopy and surface topographical analysis on 10 μm base-BOPP film showed that the film was very smooth (mean area surface roughness of 24 nm), with distinctive crater-like surface structures on one side of the film.

B. Dielectric breakdown strength

Fig. 1 exemplifies the short-term dielectric breakdown characteristics of the 10 μm base-BOPP film. Compared with literature values for high-quality capacitor BOPP films [6], [7], the BOPP films showed excellent short-term breakdown performance. At 100 °C the films exhibited only a relatively modest decrease of DC dielectric strength (~13–20%), similarly as in [4]. The large-area approach also revealed some electrical weak points which caused deviation from a single Weibull distribution in the low probability region [1], [7]. The DC small-area single-breakdown distribution resided at a slightly higher breakdown field range in comparison to large-area DC multi-breakdown data; this is attributable to the electrode area-effect, as the probability of encountering weak points decreases when the active area becomes smaller. With this considered, the breakdown data produced by the two methods were found to be in good mutual agreement. The small-area AC breakdown strength data (peak AC voltage) were found to be in similar or slightly lower range in comparison to the DC small-area breakdown data which is also consistent with literature [2].

C. Permittivity and dielectric loss

For all the studied films the relative permittivities at room temperature (1 kHz) were in the range of $\epsilon_r = 2.22$ –2.30 which

TABLE I. BREAKDOWN MEASUREMENT SPECIFICATIONS.

Method	Voltage	T (°C)	A (cm ²)	N	A_{tot} (cm ²)
Large-area MB	DC	RT	81	20	1620
Large-area MB	DC	100	81	6	486
Small-area SB	DC	RT	1	20	20
Small-area SB	AC	RT	1	20	20

RT: Room temperature: $T = 23.7^\circ\text{C} \pm 0.6^\circ\text{C}$

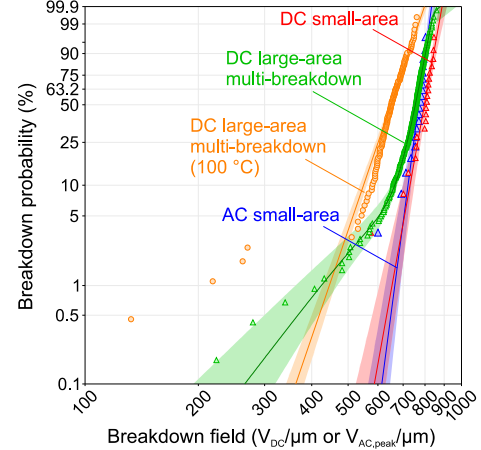


Fig. 1. Dielectric breakdown data of base-BOPP (10 μm). The shaded areas are 90 % confidence bounds.

is typical for BOPP. With increasing temperature from -60 °C up to 100 °C a slight (~5 %) decrease in ϵ_r values was observed which is consistent with Kahouli *et al* [8]. The dielectric loss behavior ($\tan \delta = \epsilon''/\epsilon'$) of the studied films is exemplified in Fig. 2 as a function of temperature and frequency, showing very low dielectric loss ($< 2 \times 10^{-4}$) around room temperature. An increase of $\tan \delta$ at low frequencies is apparent in Fig. 2, which may be related to a charge build-up originating from the electrode evaporation process. Indeed, the increase in $\tan \delta$ at low frequencies seemed to mitigate and shift to higher temperature range over time, especially when the sample was pre-conditioned at elevated temperature. In the -5 °C to 60 °C range a broad relaxation peak is seen, the onset of which is in good agreement with the measured T_g , and can hence be associated with the glass transition [8]. With increasing temperature up to 100 °C and above a strong increase in $\tan \delta$ especially at low frequencies is observed; this is likely due to the release of trapped charge and increase of DC conductivity with temperature, as will be discussed later.

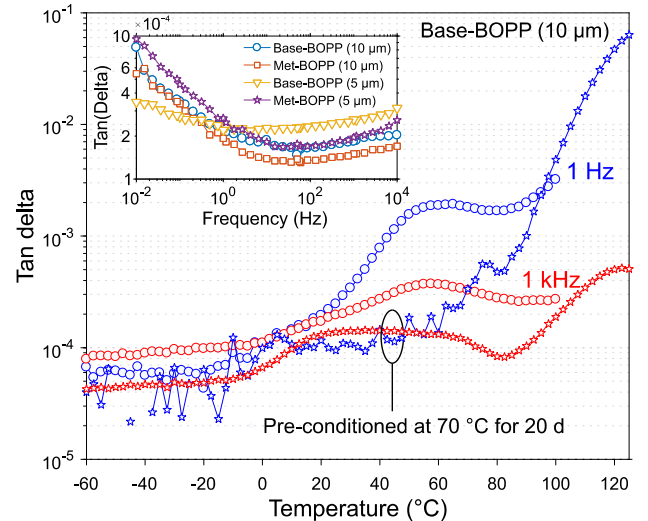


Fig. 2. $\tan \delta$ behavior of 10 μm base-BOPP as a function of temperature at 1 Hz and 1 kHz (Ni/Au evaporated electrodes). Circles: non-conditioned sample. Stars: pre-conditioned sample. Inset: Room temperature $\tan \delta$ of all the studied films as a function of frequency (non-conditioned samples).

D. TSDC

A TSDC spectra of a 10 μm base-BOPP sample is presented in Fig. 3a, with the distinctive current peaks in the low and high temperature regions suggesting the presence of shallow and deep traps, respectively. The TSDC spectra is similar to the ones presented by Li *et al.* for capacitor BOPP [9], however, it is notable that the current intensity in the shallow trap region in Fig. 3a is relative low in proportion to the strong peak in the high-temperature region (deep traps).

Thermally stimulated current arising from a single charge relaxation process can be generally expressed as:

$$I_D(T) = A \exp \left\{ -\frac{E}{kT} - \frac{B}{\beta} \int_{T_0}^T \exp \left(-\frac{E}{kT} \right) dT \right\} \quad (1)$$

where E is the trap depth, k is the Boltzmann constant, β is the heating rate (Ks^{-1}), T_0 is the initial temperature before heating and A and B are parameters which relate to charge release mechanisms as discussed in [10]. Under slow retrapping conditions, $A = P_0/\tau_0$ and $B = \nu$ where P_0 is the initial polarization, τ_0 is the relaxation time and ν is the escape frequency factor (s^{-1}). A multi-peak fitting process based on Eq. (1) was carried out to obtain a reasonable fit to the TSDC data in Fig. 3a, suggesting shallow trap states with activation energies in the 0.3–0.8 eV range which is reasonable for PP [11]. The calculated deep trap level (2.45 eV) may however be overestimated. Moreover, the issue with the curve fitting method is that the number of TSC peaks has to be assumed *a priori*. As a second approach, a modified thermally stimulated depolarization current (MTSDC) [12] was applied, allowing direct determination of the trap level and density of trap states. Fig. 3b shows the MTSDC analysis around the glass-transition region, indicating a shallow trap level of ~ 0.75 eV. The deep traps resided around 1.08 eV (not shown). Such trap levels, which may be associated with impurities or chemical defects such as carbonyl, conjugated double bonds and dienone [13] present in the PP, will have an impact on dielectric properties.

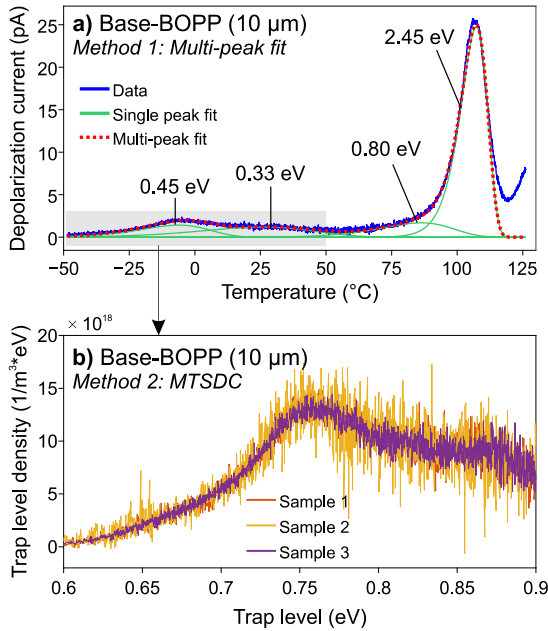
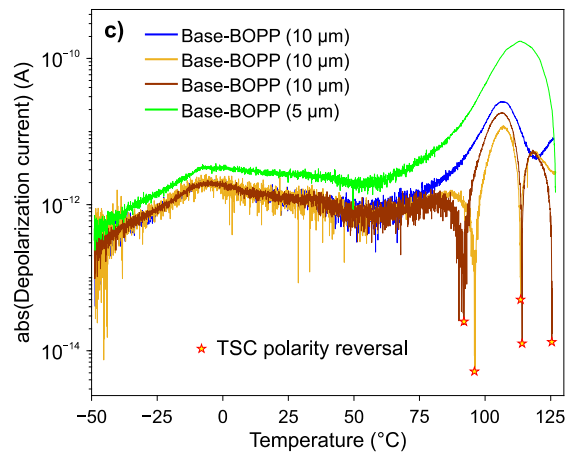


Fig. 3. a) Thermally stimulated depolarization current measured from a 10 μm base-BOPP film sample with evaporated Ni/Au electrodes ($E_p = 100 \text{ V}/\mu\text{m}$). Multi-peak fitting based on Equation (1) has been carried out and the trap levels corresponding to each peak are labelled. **b)** Trap level and density analysis of the shallow trap region in a) according to modified thermally stimulated depolarization current (MTSDC) theory. **c)** TSDC spectra of several base-BOPP film samples (5 and 10 μm) exemplifying the anomalous TSC behavior in the high-temperature region (deep traps) which was observed for some of the samples ($E_p = 100 \text{ V}/\mu\text{m}$). The depolarization current (y-axis) is represented as absolute values in order to use logarithmic scale. TSC polarity reversals are labelled.

Fig. 3c illustrates polarity reversal and anomalous TSC behavior (i.e. current which is flowing in the same direction as charging current) which were sometimes observed in the high temperature region. The anomalous TSC behavior is likely associated with space charge effects, influenced by the nature of the electrical contacts (i.e. ohmic vs. blocking contacts) [14]. A more detailed analysis will be presented elsewhere.

E. DC conductivity

Fig. 4a–c present the averaged conductivity vs. total experiment time for the 10 μm base-BOPP film with evaporated Ni/Au electrodes at different temperatures and electric fields. The measured conduction currents showed long-term power-law decay ($\sim t^{-n}$) with the exponent n varying roughly between 0.2 and 0.6, in agreement with Ghorbani *et al.* [15]. Increasing temperature from 30 $^{\circ}\text{C}$ to 100 $^{\circ}\text{C}$ was found to increase the conductivity from roughly $4.4 \times 10^{-17} \text{ S/m}$ to $6.3 \times 10^{-16} \text{ S/m}$. Surprisingly, the measured conductivities did not show a clear dependency on electric field magnitude in the 30–250 $\text{V}/\mu\text{m}$ range studied, but rather, the conductivity showed a slowly decreasing and saturating trend over time (Fig. 4d). This is in contrast with Ho *et al.* [4] who report a non-linear field-dependent conductivity increase for a 7 μm tetter BOPP capacitor film above a threshold field of 100 $\text{V}/\mu\text{m}$ (also measured under progressively increasing electric field). On the other hand, weak field-dependence of BOPP film conductivity up to ~ 250 –400 $\text{V}/\mu\text{m}$ range is not unprecedented [15]–[17], and such differences could be attributed to differences in e.g. film manufacturing process, morphology and base polymer purity. Here, the relatively low shallow trap density along with a high deep trap density is notable from the TSDC measurements—such an electronic structure, which may be thought to suppress charge hopping between shallow trap sites and block further charge injection due to the formation of homocharge layers at the electrode–BOPP interface, could indeed explain the very low conductivity values measured. However, ultimately, it is important to consider the fact that the electrode evaporation process itself is likely resulting in modification of the physical,



chemical and electrical properties in the BOPP-metal interface [14], and hence, the measured properties cannot be directly associative with BOPP alone. The possible effects of slow morphological changes during the measurement (e.g. secondary crystallization at elevated temperatures) also need to be considered carefully. Further work is ongoing to study these effects in more detail, also at higher fields.

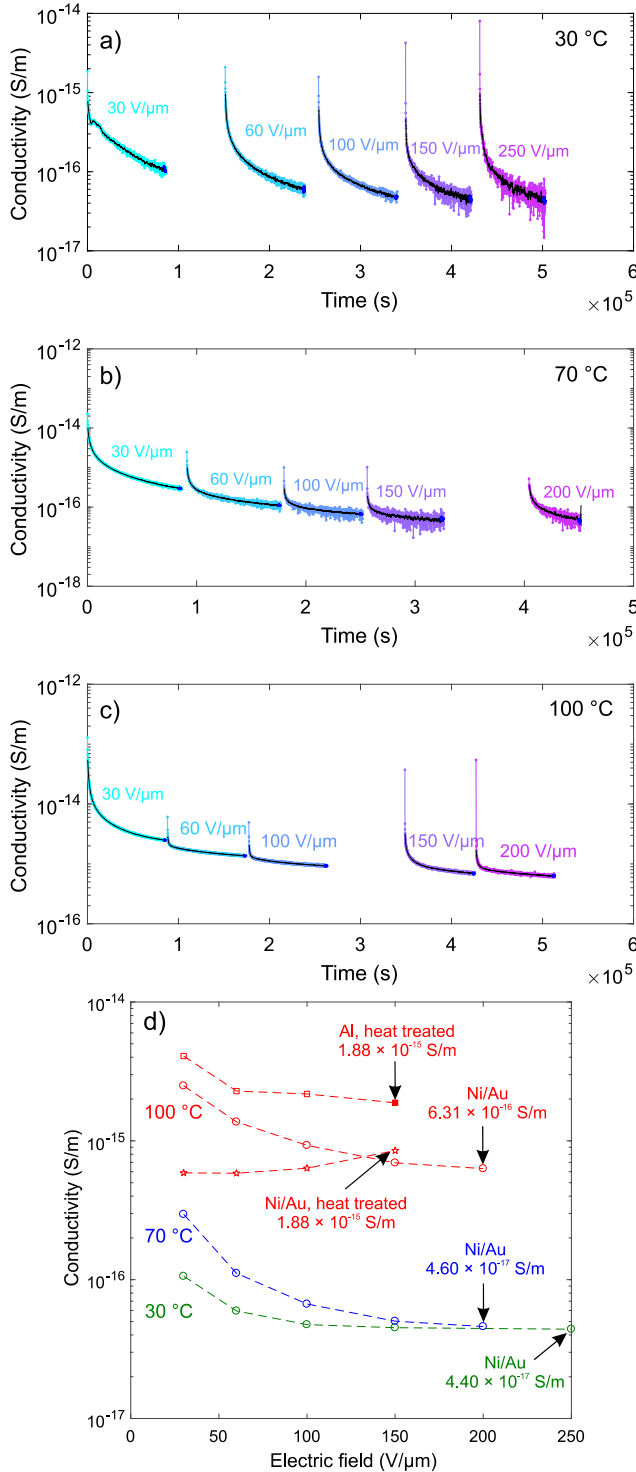


Fig. 4. Averaged conductivity vs. experiment time for 10 μm base-BOPP film with evaporated Ni/Au electrodes at **a)** 30 $^{\circ}\text{C}$, **b)** 70 $^{\circ}\text{C}$ and **c)** 100 $^{\circ}\text{C}$ under progressively increasing DC voltage stress. A generalized moving average filter (Savitzky-Golay filter) was applied to smooth the data (solid black lines). **d)** Averaged conductivity at the end of each 20–24 h voltage application period. Additional data from heat treated samples with either Ni/Au or Al electrodes are also shown. The filled marker at 100 $^{\circ}\text{C}$ corresponds to a fresh sample with no prior electrical stress subjected to 150 $\text{V}/\mu\text{m}$ field for ~ 51 h.

IV. CONCLUSIONS

The studied commercial BOPP capacitor films exhibited high dielectric breakdown performance, low dielectric loss characteristics and very low electrical conductivity which may be associated with the density and depth distribution of charge trap states in the films. However, further studies are still needed to elucidate the role of electrodes in the observed dielectric phenomena. Future work involving incorporation of nanoparticles in BOPP may result in interesting dielectric property modifications (e.g. changes in charge trapping properties), especially at high temperatures.

ACKNOWLEDGMENT

This project has received funding from the European Union's Horizon 2020 research and innovation program under grant agreement No 720858.

REFERENCES

- [1] I. Rytöluoto, K. Lahti, M. Karttunen, and M. Koponen, "Large-area dielectric breakdown performance of polymer films—Part I: Measurement method evaluation and statistical considerations on area-dependence," *IEEE Trans. Dielectr. Electr. Insul.*, vol. 22, no. 2, 2015.
- [2] M. Ritamäki, I. Rytöluoto, M. Niittymäki, K. Lahti, and M. Karttunen, "Differences in AC and DC large-area breakdown behavior of polymer thin films," in *2016 IEEE Int. Conf. Dielectr.*, pp. 1011–1014, 2016.
- [3] M. Ritamäki, I. Rytöluoto, and K. Lahti, "High temperature and ageing test methods to characterize the dielectric properties of BOPP capacitor films," in *2017 IEEE Conf. Electr. Insul. Dielectr. Phen.*, 2017, pp. 266–269.
- [4] J. Ho and T. R. Jow, "High field conduction in biaxially oriented polypropylene at elevated temperature," *IEEE Trans. Dielectr. Electr. Insul.*, vol. 19, no. 3, pp. 990–995, 2012.
- [5] I. Rytöluoto, A. Gitsas, S. Pasanen, and K. Lahti, "Effect of film structure and morphology on the dielectric breakdown characteristics of cast and biaxially oriented polypropylene films," *Eur. Polym. J.*, vol. 95, 2017.
- [6] C. Xu, J. Ho, and S. A. Boggs, "Automatic breakdown voltage measurement of polymer films," *IEEE Electr. Insul. Mag.*, vol. 24, no. 6, pp. 30–34, 2008.
- [7] S. J. Laihonon, U. Gäfvert, T. Schütte, and U. W. Gedde, "DC breakdown strength of polypropylene films: Area dependence and statistical behavior," *IEEE Trans. Dielectr. Electr. Insul.*, vol. 14, no. 2, pp. 275–286, 2007.
- [8] A. Kahouli, O. Gallot-Lavallée, P. Rain, O. Lesaint, C. Guillermin, and J.-M. Lupin, "Dielectric features of two grades of bi-oriented isotactic polypropylene," *J. Appl. Polym. Sci.*, vol. 132, no. 28, p. 42224, 2015.
- [9] H. Li *et al.*, "Study on the impact of space charge on the lifetime of pulsed capacitors," *IEEE Trans. Dielectr. Electr. Insul.*, vol. 24, no. 3, pp. 1870–1877, Jun. 2017.
- [10] Y. Wang, J. Wu, and Y. Yin, "A modified thermally stimulated current analysis method for direct determination of trap energy distribution," *IEEE Trans. Dielectr. Electr. Insul.*, vol. 24, no. 5, pp. 3138–3143, 2017.
- [11] G. Mazzanti and M. Marzinotto, *Extruded Cables for High-Voltage Direct-Current Transmission: Advances in Research and Development*. Wiley-IEEE Press, 2013.
- [12] F. Tian, W. Bu, L. Shi, C. Yang, Y. Wang, and Q. Lei, "Theory of modified thermally stimulated current and direct determination of trap level distribution," *J. Electrostat.*, vol. 69, no. 1, pp. 7–10, Feb. 2011.
- [13] H.-V. Nguyen and T. H. Pham, "Structural and Electronic Properties of Defect-Free and Defect-Containing Polypropylene: A Computational Study by van der Waals Density-Functional Method," *Phys. Status Solidi*, vol. 1700036, p. 1700036, Oct. 2017.
- [14] A. Thielen, J. Niezette, G. Feyder, and J. Vanderschueren, "Thermally stimulated current study of space charge formation and contact effects in metal-polyethylene terephthalate film-metal systems. I. Generalities and theoretical model," *J. Phys. Chem. Solids*, vol. 57, no. 11, pp. 1567–1580, 1996.
- [15] H. Ghorbani *et al.*, "Long-term conductivity decrease of polyethylene and polypropylene insulation materials," *IEEE Trans. Dielectr. Electr. Insul.*, vol. 24, no. 3, pp. 1485–1493, Jun. 2017.
- [16] Zongze Li, H. Uehara, R. Ramprasad, S. Boggs, and Yang Cao, "Pre-breakdown conduction in polymeric films," in *2015 IEEE Conf. Electr. Insul. Dielectr. Phen.*, 2015, pp. 872–875.
- [17] X. Qi, Z. Zheng, and S. Boggs, "Engineering with nonlinear dielectrics," *IEEE Electr. Insul. Mag.*, vol. 20, no. 6, pp. 27–34, 2004.